SUPPLEMENTARY INFORMATION

Table S1. Putative interacting proteins of GluN1 identified by mass spectrometric analysis of a protein sample immunopurified with anti-GluN1 antibody from rat brains.

Protein UniProt ID (Rat)	# unique peptides	# total peptides	Total score	emPAI
NMDZ1	**41**	**155**	**3461**	**3.61**
TBB2B	9	63	1190	0.89
NMD3A	**14**	**32**	**757**	**0.5**
TBB3	8	26	561	0.66
GEPH	8	15	503	0.36
NMDE2	**11**	**23**	**450**	**0.26**
CSKI1	7	12	381	0.16
CALX	8	15	371	0.46
NMDE1	**8**	**15**	**357**	**0.17**
K2C73	5	9	244	0.3
IRK4	6	14	242	0.47
K2C75	6	9	177	0.39
NFH	4	6	174	0.12
HS90B	3	4	133	0.12
DYN1	3	4	128	0.1
CBS	1	2	120	0.05
NMDE3	**2**	**4**	**114**	**0.05**
LYRIC	4	4	100	0.22
AT2A2	5	7	99	0.15
EF1A2	3	5	92	0.21
MPRIP	1	2	91	0.03
SH3K1	2	4	89	0.09
SPON1	2	4	87	0.07
CH60	2	2	86	0.11
GRIA2	4	4	81	0.14
SND1	6	7	80	0.21
SNG1	1	2	74	0.13
UXS1	2	3	70	0.14
SCN2A	3	5	68	0.06
VDAC2	2	2	68	0.22
VGLU1	1	1	68	0.05
NFASC	3	5	68	0.07
AT2B2	3	4	66	0.07
SYT2	2	3	64	0.14
IRK12	2	5	63	0.14
CPSF7	1	2	62	0.06
KCMA1	**1**	**1**	**59**	**0.02**
DC1I1	1	1	56	0.05
ANXA2	1	1	54	0.09
VATB2	1	1	52	0.06
RL15	1	1	51	0.14

Only proteins of those with a mascot score of ≥ 50, which were not detected in the negative control sample, are listed. Proteins of NMDA receptors and BK channels are shown highlighted in bold. The number of unique peptides was calculated as the number of nonredundant peptide sequences specifically belonging to the indicated protein. The total score of a protein was calculated as a sum of scores of all the peptides having scores above the "identity" threshold given by Mascot. The Exponentially Modified Protein Abundance Index (emPAI) was considered a rough estimation of the relative protein abundances. Its calculation followed what had been described in (1).

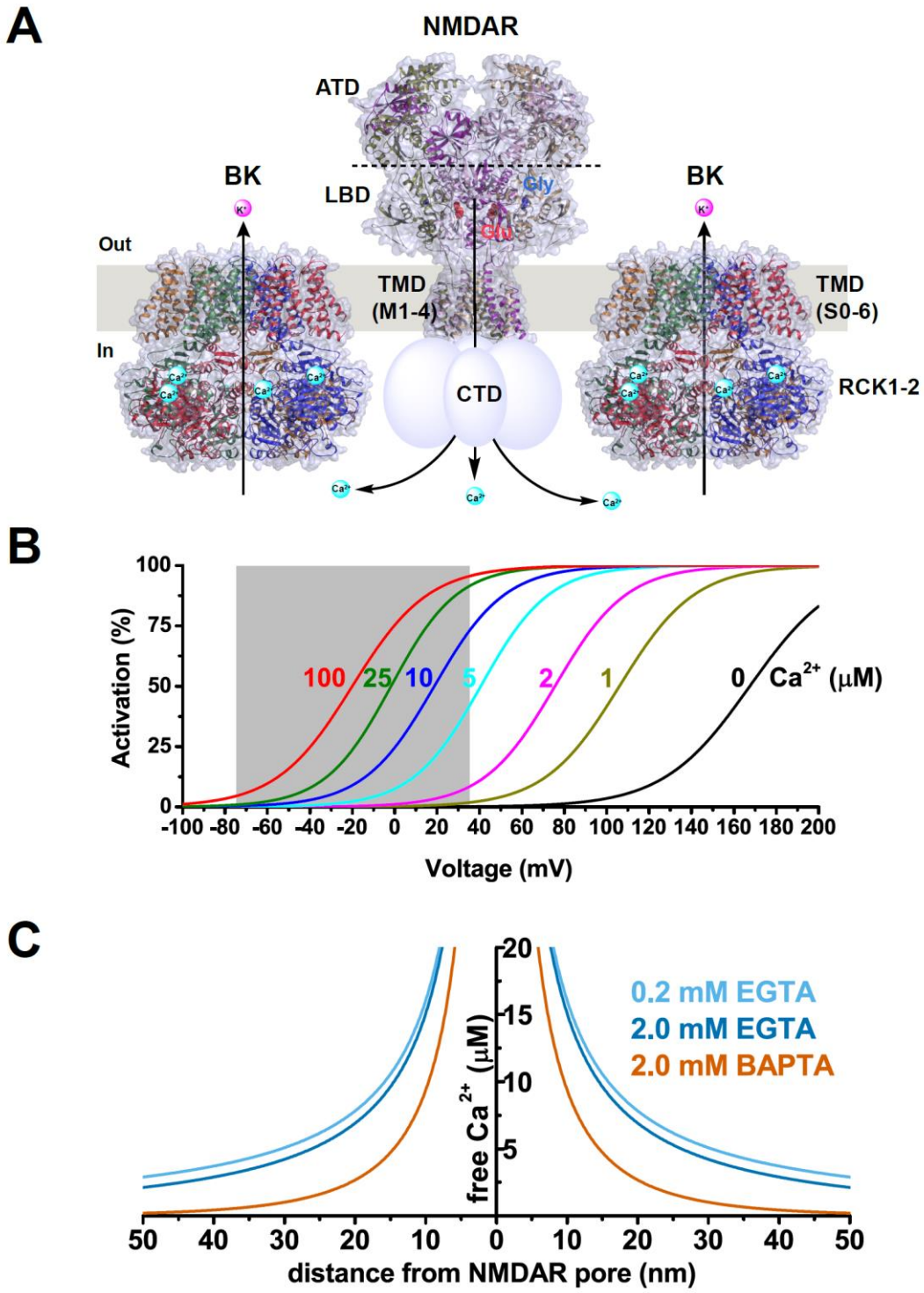

Fig. S1. NMDAR-mediated BK channel activation requires short-distance coupling between these two channels. (***A***) Structural models and Ca^{2+}-mediated functional coupling of the BK channel and NMDAR within a nanodomain. Structures were redrawn from published structures (2, 3). The amino terminal domain (ATD), ligand binding domain (LBD), transmembrane domain (TMD), and C-terminal domain (CTD) are indicated on or near the corresponding structural parts. (***B***) Voltage and Ca^{2+} dependence of BKα channel activation. The shaded area indicates a physiological range of membrane voltages. (***C***) Predicted distance dependence of the local free Ca^{2+} concentration originating from an NMDAR channel pore in the presence of 0.2 and 2 mM EGTA or 2 mM BAPTA. Prediction was performed using the CalC software (version 6.8.0) (4) at 0.1 pA for the NMDAR single-channel Ca^{2+} current (estimated at about -20 mV). Chelator and Ca^{2+} parameters were taken from previous reports (5-7).

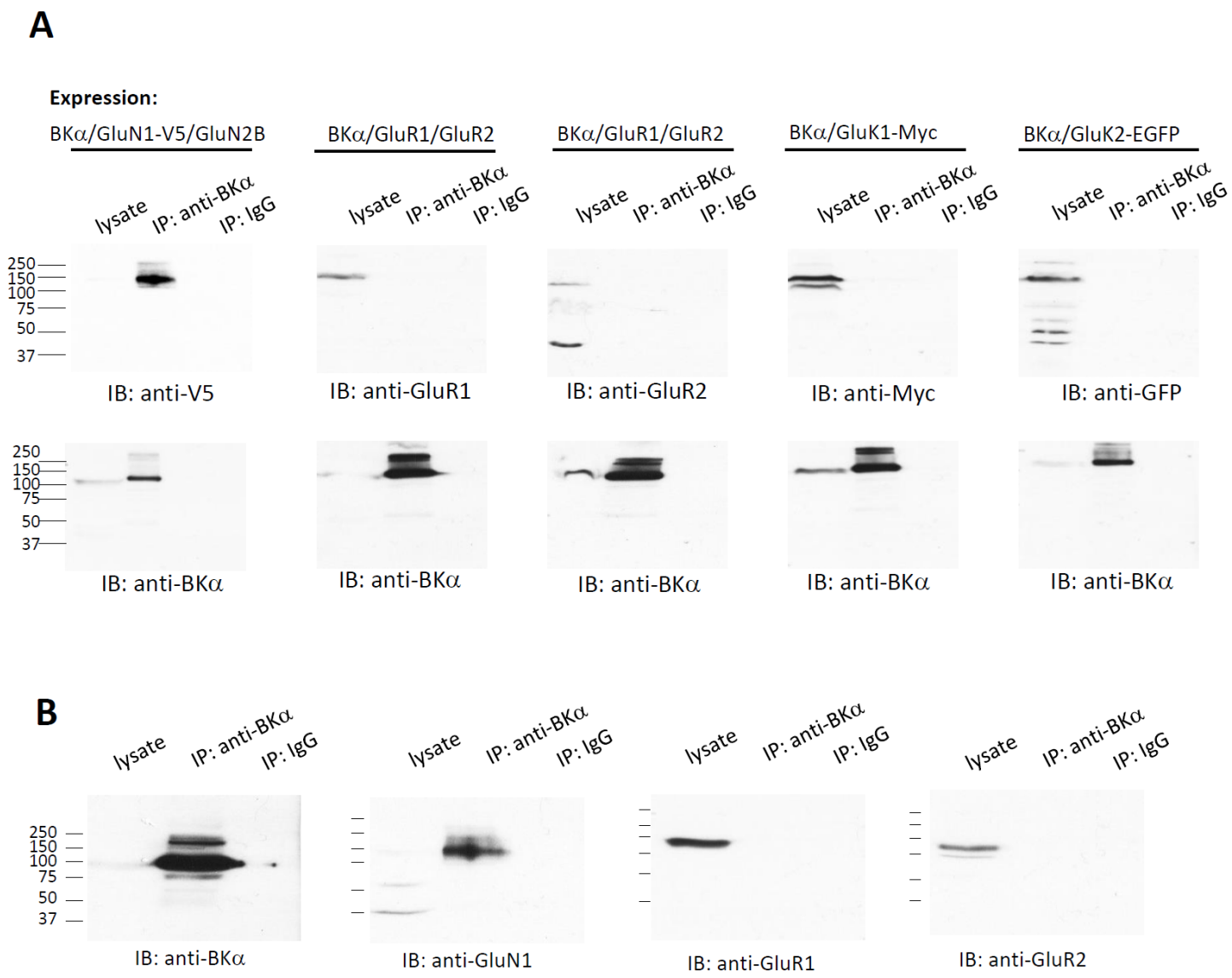

Fig. S2. The BKα channel was unable to interact with non-NMDA ionotropic glutamate receptors. (***A***) Immunopurification and immunoblot (IB) analysis of BK channels and ionotropic glutamate receptors co-expressed in the heterologous expression system of HEK-293 cells. IP, immunopurification; GFP, green fluorescent protein. (***B***) Immunopurification and immunoblot analysis of BK channels and AMPA receptors in rat brains. BK channel complexes were immunopurified with an anti-BKα antibody and then immunoblotted with different antibodies to identify the co-purified glutamate receptor proteins (recombinant or native).

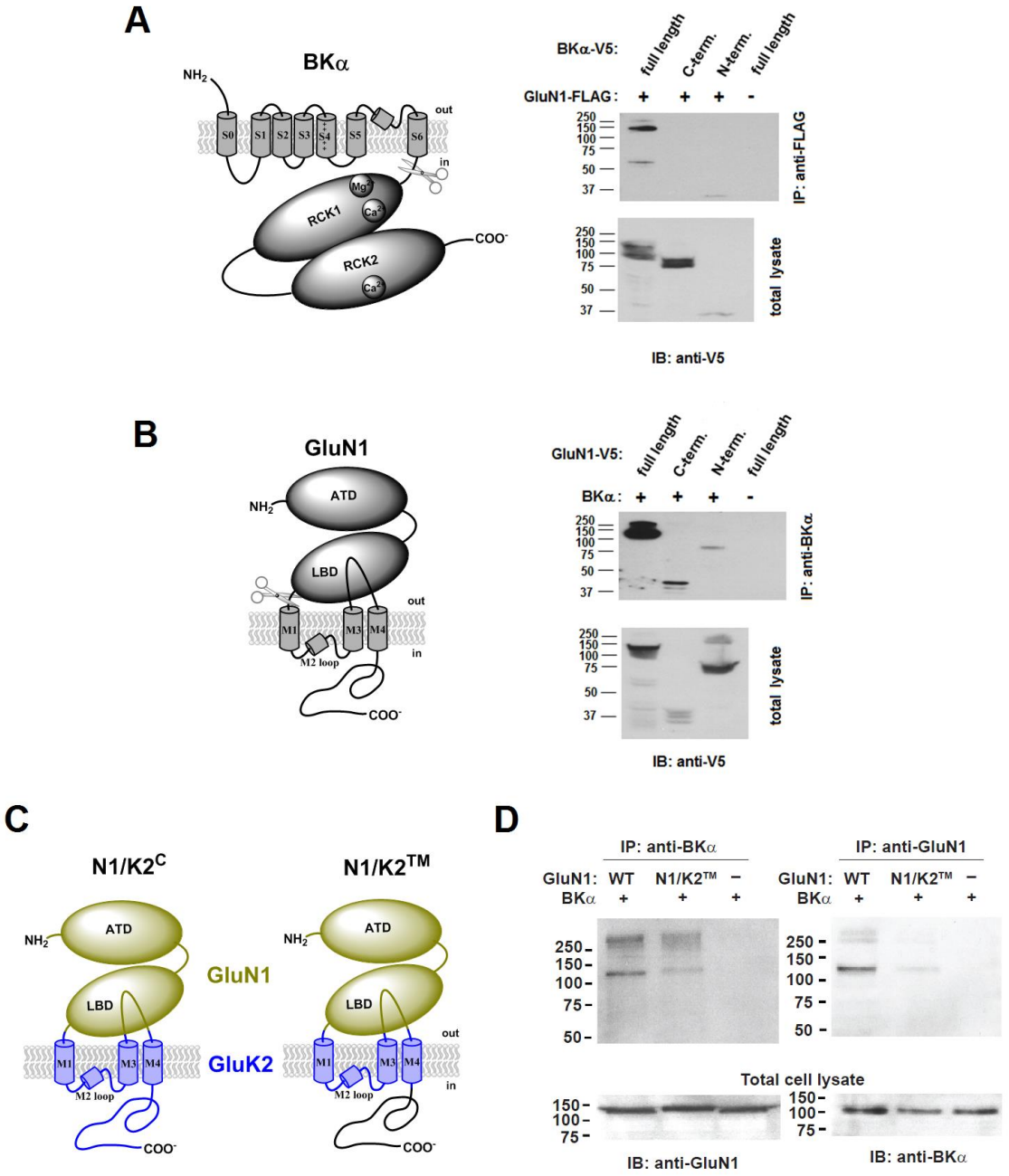

Fig. S3. BKα and GluN1 likely interact with each other via their N-terminal part and C-terminal part, respectively. (***A***) GluN1 interacts with the BKα's N-terminal part but not its C-terminal part. FLAG-tagged GluN1 was co-expressed with the full-length, N-terminal (term.) part (residues 1-324) or C-terminal part (residues 325-1113) of V5-tagged BKα in HEK-293 cells, immunoprecipitated (IP) with an anti-FLAG antibody, and immunoblotted (IB) with an anti-V5 antibody to detect the co-immunoprecipitated BKα protein. The topology of BKα and the splitting sites (scissor) of the N-terminal and C-terminal constructs are depicted on the left side. (***B***) BKα interacts with the GluN1's C-terminal part more effectively than its N-terminal part. BKα was co-expressed with the full-length, N-terminal part (residues 1-541), or C-terminal part (residues 542-920) of V5-tagged GluN1 in HEK-293 cells, IP with an anti-BKα antibody, and IB with an anti-V5 antibody to detect the co-immunoprecipitated GluN1 protein. The topology of GluN1 and the splitting sites (scissor) of the N-terminal and C-terminal constructs are depicted on the left side. (***C***) The topologic depiction of GluN1 and GluK2 chimeric constructs. (***D***) Reciprocal pull-down assay showed that the association between BKα and GluN1 was compromised with the GluN1 N1/K2^{TM} mutant in which the TM region was replaced by that of GluK2.

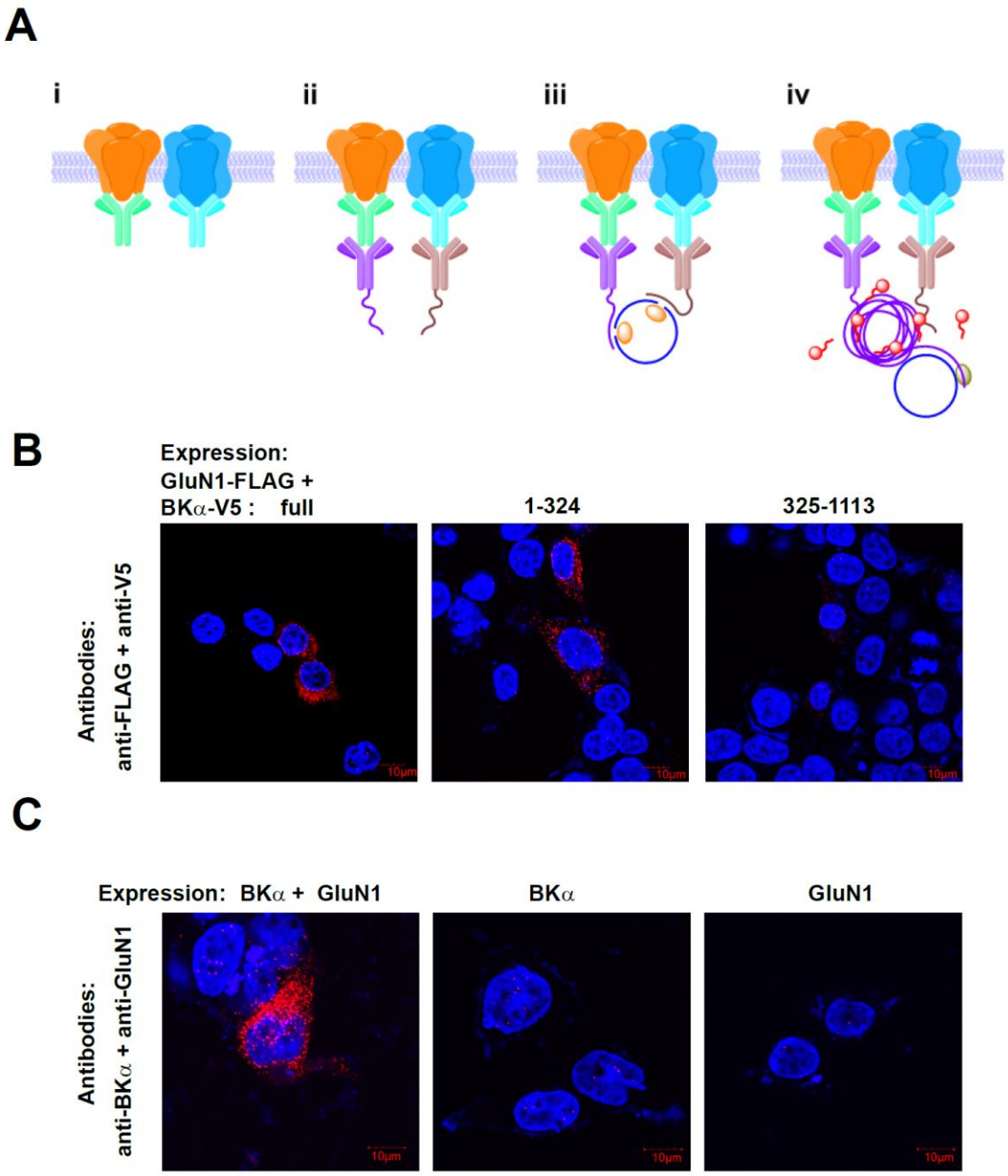

Fig. S4. *In situ* PLA of BK-NMDAR complexes in HEK-293 cells. (***A***) Schematic of the *in situ* PLA. (i) Specific primary antibodies are used to bind each channel. (ii) Secondary species-specific antibodies conjugated with oligonucleotides (PLA probes PLUS and MINUS) recognize primary antibodies. (iii) Two oligonucleotides (blue) are added to hybridize with the PLA probes to form an open circular single-stranded DNA if the two epitopes for primary antibodies are in close proximity (<40 nm). T4 ligase (orange oval) is used to close the circular single-stranded DNA. (iv) Phi29 DNA polymerase (olive oval) is used to extend the single-stranded DNA via rolling-circle amplification using one of the PLA probes as a primer. The concatemeric product is detected by hybridization with fluorescent oligonucleotide probes (red). (***B***) PLA signals probed with anti-V5 and anti-FLAG antibodies were strong in HEK-293 cells co-expressing FLAG-tagged GluN1 and BKα-V5's full-length construct or N-terminal TM domain construct (residues 1-324) but very weak in cells expressing BKα-V5's C-terminal intracellular domain construct (residues 325-1113). (***C***) Strong PLA signals (red dots) probed with anti-BKα and anti-GluN1 antibodies were detected in HEK-293 cells expressing both BKα and GluN1 but not in those expressing BKα or GluN1 alone. The point-like PLA signal represents a single or, more likely, a cluster of BKα-GluN1 complex(es).

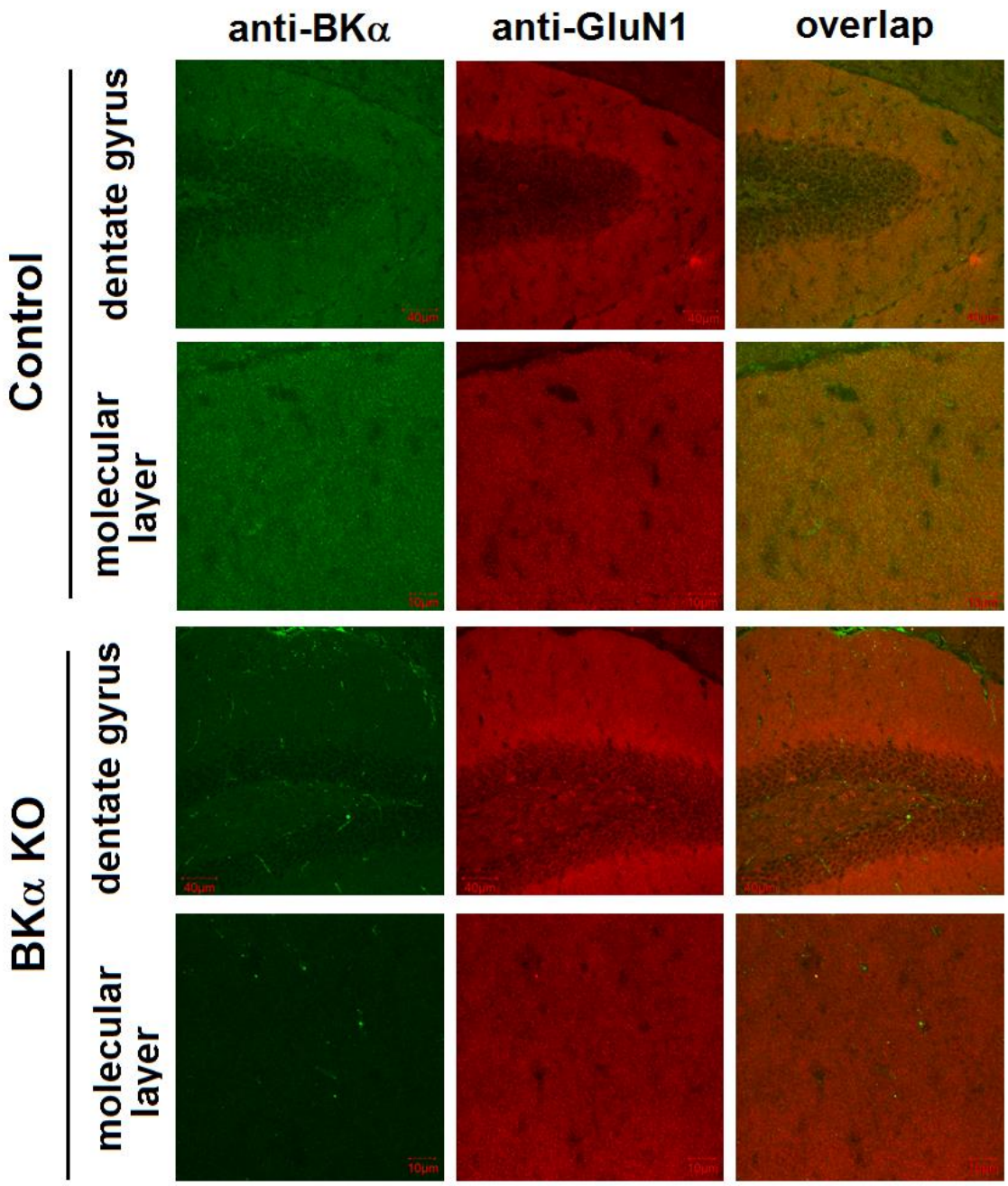

Fig. S5. Immunofluorescent labeling of BKα and GluN1 in the mouse dentate gyrus. Control and BKα KO are F2 Nestin-Cre^{-} and Nestin-Cre^{+} mice with a homozygous genotype of KCNMA1$^{fl/fl}$, i.e., Nestin-Cre^{-}/KCNMA1$^{fl/fl}$ and Nestin-Cre^{+}/KCNMA1$^{fl/fl}$, respectively. The antibodies used are same as those used in Fig. 3 and Supplementary Fig. 4C. The mouse monoclonal antibody (NeuroMab) and the anti-GluN1 antibody (EMD Millipore) were both used at 1:100 dilution.

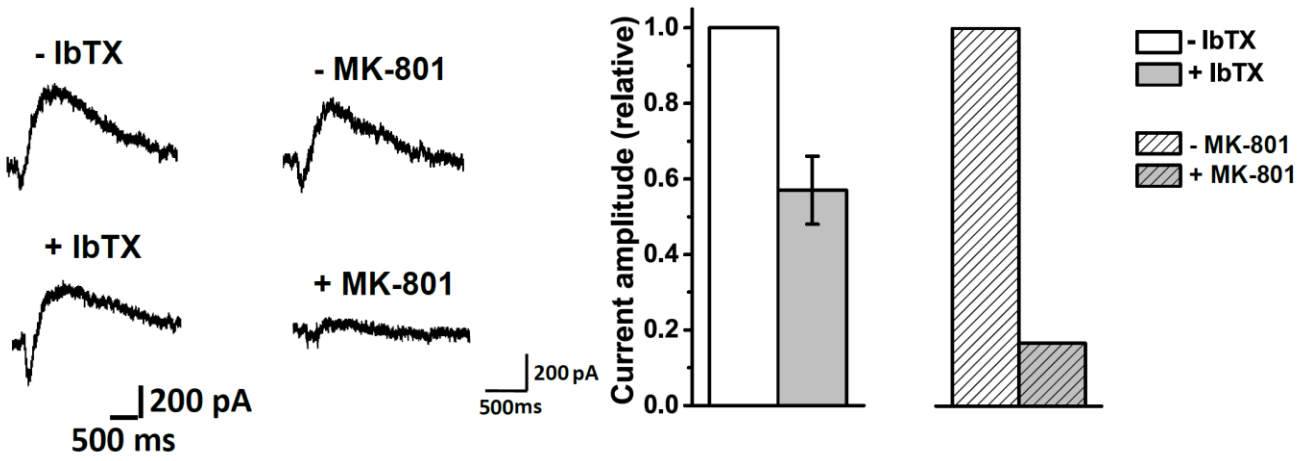

Fig. S6. Effects of IbTX and MK-801 on glutamate-induced outward currents in dentate gyrus granule cells. IbTX at 250 nM (n = 3) and MK-801 at 10 μM (n =2) were perfused into the bath solution for 15 and 10 min, respectively, before data recording.

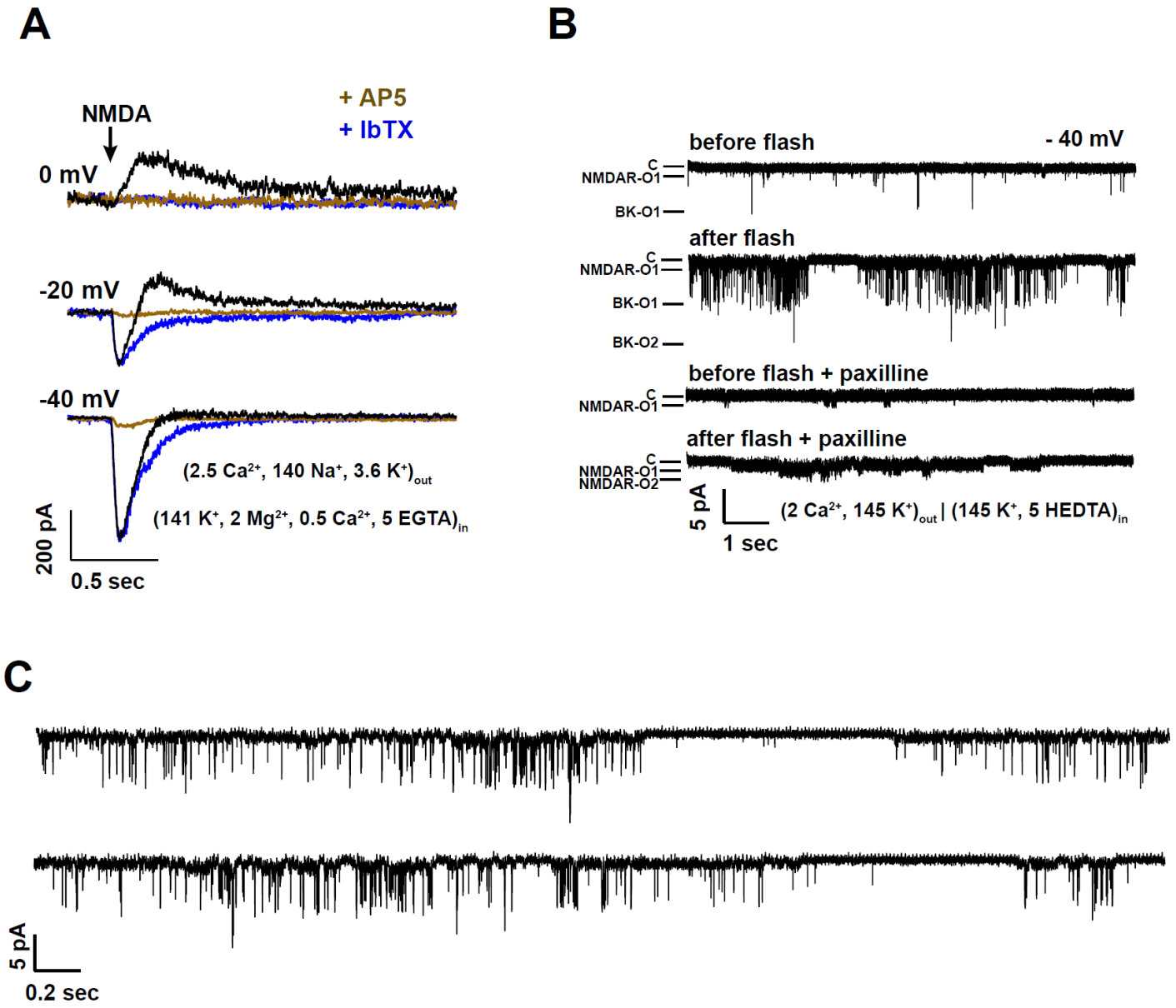

Fig. S7. BK channel activation by NMDAR (GluN1/GluN2A)-mediated Ca^{2+} influx in HEK-293 cells. (***A***) Whole-cell patch-clamp recording of BK channel and NMDAR currents over the course of application of NMDA (300 μM for 50 ms) alone and together with AP5 (100 μM for 50 ms) or IbTX (1 μM with preincubation for 5 min). BKα, GluN1, and GluN2A were expressed in HEK-293 cells. A bath solution containing 140 mM NaCl, 3.6 mM KCl, 2.5 mM $CaCl_2$, and 20 mM HEPES (pH 7.2) with and without the drugs was continuously perfused onto the cells using a pressurized perfusion system. Pipette electrodes were filled with a solution containing 141 mM $KMeSO_3$, 0.5 mM $CaCl_2$, 5 mM EGTA, and 20 mM HEPES (pH 7.2). For comparison, currents obtained with IbTX at -20 mV and -40 mV were normalized according to those without drug treatment at peak amplitudes. (***B***) Single-channel traces of BK channels and NMDARs at -40 mV before and after flash photolysis of caged NMDA in an excised inside-out patch. The excised patch was recorded in symmetric K^+ recording solutions of 145 mM $KMeSO_3$ and 20 HEPES (pH 7.2) supplemented with 2 mM $CaCl_2$ on the extracellular side and 5 mM N-(2-Hydroxyethyl)ethylenediaminetriacetic acid (HEDTA) on the intracellular side. NMDAR activation was induced by flash photolysis (10 ms) of caged NMDA (3 mM) in the pipette electrode solution using an ultraviolet light guide (950 μm in diameter) coupled with a high-power 365-nm ultraviolet light-emitting diode (Rapp OptoElectronic). Paxilline (10 μM; preincubated for 5 min) was used to block BK channels. (***C***) Expanded view of the "after flash" single-channel trace in ***B***.

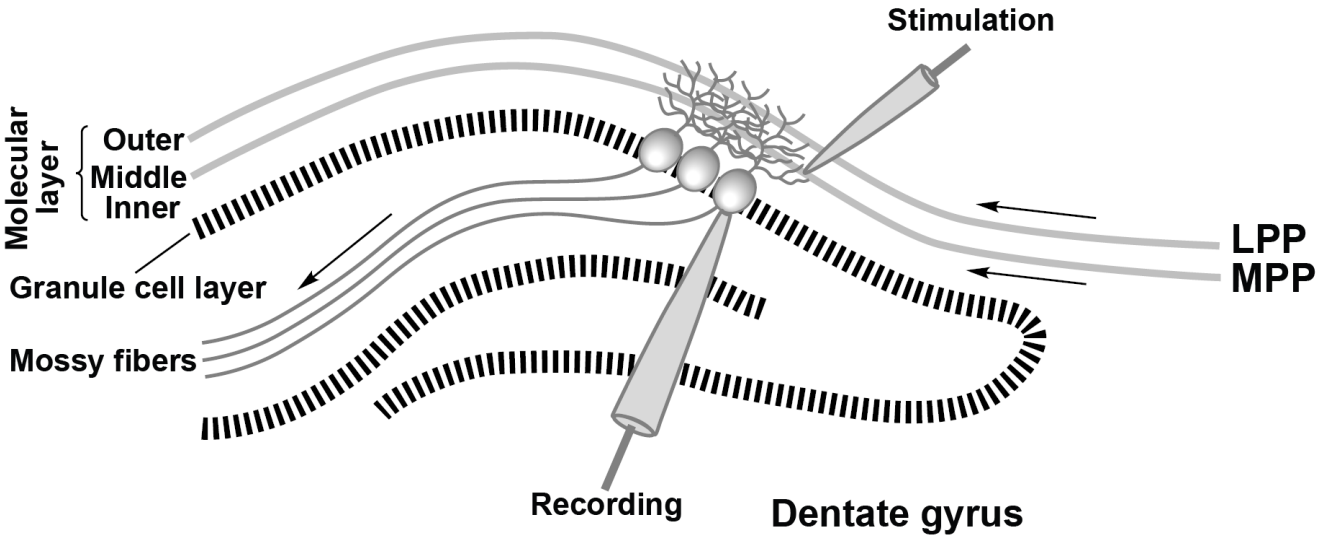

Fig. S8. Schematic of the dentate gyrus and experimental configuration for whole recording of evoked EPSPs or EPSCs of dentate granule cells by stimulation of the MPP in the middle of the molecular layer. LPP, lateral perforant path.

REFERENCES

1. Ishihama Y, *et al.* (2005) Exponentially modified protein abundance index (emPAI) for estimation of absolute protein amount in proteomics by the number of sequenced peptides per protein. *Mol Cell Proteomics* 4(9):1265-1272.
2. Tao X, Hite RK, & MacKinnon R (2017) Cryo-EM structure of the open high-conductance Ca^{2+}-activated K^{+} channel. *Nature* 541(7635):46-51.
3. Karakas E & Furukawa H (2014) Crystal structure of a heterotetrameric NMDA receptor ion channel. *Science* 344(6187):992-997.
4. Matveev V, Zucker RS, & Sherman A (2004) Facilitation through buffer saturation: constraints on endogenous buffering properties. *Biophys J* 86(5):2691-2709.
5. Naraghi M & Neher E (1997) Linearized buffered Ca^{2+} diffusion in microdomains and its implications for calculation of $[Ca^{2+}]$ at the mouth of a calcium channel. *J Neurosci* 17(18):6961-6973.
6. Fakler B & Adelman JP (2008) Control of K(Ca) channels by calcium nano/microdomains. *Neuron* 59(6):873-881.
7. Eggermann E, Bucurenciu I, Goswami SP, & Jonas P (2011) Nanodomain coupling between Ca^{2+} channels and sensors of exocytosis at fast mammalian synapses. *Nat Rev Neurosci* 13(1):7-21.